The Journal of Experimental Biology 204, 1369–1379 (2001)
Printed in Great Britain © The Company of Biologists Limited 2001
JEB3384

SLOW MUSCLE POWER OUTPUT OF YELLOW- AND SILVER-PHASE EUROPEAN EELS (*ANGUILLA ANGUILLA* L.): CHANGES IN MUSCLE PERFORMANCE PRIOR TO MIGRATION

D. J. ELLERBY[1,*], I. L. Y. SPIERTS[2] AND J. D. ALTRINGHAM[1]

[1]*School of Biology, University of Leeds, Leeds LS2 9JT, UK* and [2]*Niels Stensen Foundation, PO Box 20111, 1000HC Amsterdam, The Netherlands*

*e-mail: bgydje@leeds.ac.uk

Accepted 25 January; published on WWW 15 March 2001

Summary

Eels swim in the anguilliform mode in which the majority of the body axis undulates to generate thrust. For this reason, muscle function has been hypothesised to be relatively uniform along the body axis relative to some other teleosts in which the caudal fin is the main site of thrust production. The European eel (*Anguilla anguilla* L.) has a complex life cycle involving a lengthy spawning migration. Prior to migration, there is a metamorphosis from a yellow (non-migratory) to a silver (migratory) life-history phase. The work loop technique was used to determine slow muscle power outputs in yellow- and silver-phase eels. Differences in muscle properties and power outputs were apparent between yellow- and silver-phase eels. The mass-specific power output of silver-phase slow muscle was greater than that of yellow-phase slow muscle. Maximum slow muscle power outputs under approximated *in vivo* conditions were 0.24 W kg^{-1} in yellow-phase eel and 0.74 W kg^{-1} in silver-phase eel. Power output peaked at cycle frequencies of 0.3–0.5 Hz in yellow-phase slow muscle and at 0.5–0.8 Hz in silver-phase slow muscle. The time from stimulus offset to 90 % relaxation was significantly greater in yellow- than in silver-phase eels. The time from stimulus onset to peak force was not significantly different between life-history stages or axial locations. Yellow-phase eels shifted to intermittent bursts of higher-frequency tailbeats at a lower swimming speed than silver-phase eels. This may indicate recruitment of fast muscle at low speeds in yellow-phase eels to compensate for a relatively lower slow muscle power output and operating frequency.

Key words: European eel, *Anguilla anguilla*, work loop technique, power, muscle, swimming.

Introduction

The European eel (*Anguilla anguilla* L.) has a complex life cycle that includes a lengthy spawning migration. Several years are spent in the non-migratory yellow phase in fresh or brackish water (Colombo and Rossi, 1978; Vøllestad and Jonsson, 1986). There follows a metamorphosis to the migratory silver phase. Eels in this phase leave fresh or brackish water in late summer or autumn (Lowe, 1952; Vøllestad et al., 1986; Poole et al., 1990). They then migrate to the Sargasso Sea, a body of warm water located in the Atlantic Ocean, where they spawn (McCleave et al., 1987). After hatching, the elvers migrate to Europe, where they leave the sea and enter fresh water (e.g. Deelder, 1958). A higher level of swimming performance in terms of sustained swimming speed and muscle power output may be required to undertake this migration.

The lateral myotomal muscle provides the power for swimming in most fish. Muscular contraction, the interactions of the fish with the water and the mechanical properties of the passive components of the body combine to produce a wave of curvature that passes along the fish from head to tail. This body/tail wave generates the thrust that propels the fish. Swimming styles based on body waves are classified on the basis of the proportion of the body contributing to thrust generation (Breder, 1926). The study of eel locomotion has a long history, and the movement of the waves of curvature along the body of an eel was first recorded photographically in 1895 (Marey, 1895). The genus *Anguilla* lends its name to anguilliform locomotion, a swimming style in which most of the length of an elongated undulatory body transfers thrust to the water. Anguilliform swimming is found in a range of phyla with elongate body forms (e.g. Gray, 1933; Graham et al., 1987; Jayne, 1988; Frolich and Biewener, 1992; for a review, see Gillis, 1996).

The lateral muscle fibres lengthen and shorten rhythmically during steady swimming. Patterns of muscle strain and activation show some variation both among species and with position along the body in a given species (Grillner and Kashin, 1976; Williams et al., 1989; van Leeuwen et al., 1990; Wardle

and Videler, 1993; Johnson et al., 1994; Jayne and Lauder, 1995; Hammond et al., 1998; Gillis, 1998b; Gillis, 2000; Ellerby et al., 2000). Studies of isolated muscle fibres from a number of fish species have shown that the phase relationship between strain and activation is crucial in determining how muscle functions (Altringham et al., 1993; Rome et al., 1993; Wardle et al., 1995; Curtin and Woledge, 1996; Hammond et al., 1998; Altringham and Ellerby, 1999).

The lateral musculature is divided into a series of metamerically arranged myotomes. In fish, different muscle fibre types with distinct properties are usually arranged in discrete populations. This facilitates study of the function of different fibre types during locomotion. Low-tailbeat-frequency sustained swimming is powered by slow-twitch, aerobic muscle (e.g. Bone, 1966; Rayner and Keenan, 1967; Rome et al., 1992; Coughlin and Rome, 1999). Fast-twitch fibres are recruited during fast starts and bursts of high-tailbeat-frequency unsustained swimming (e.g. Rayner and Keenan, 1967; Johnston et al., 1977). In eels, as in most teleosts, the slow-twitch muscle is present as a wedge positioned along the lateral line.

Anguilliform swimmers are thought to transfer thrust to the water relatively uniformly along the majority of the body axis. This is in contrast to fish with stiffer bodies and oscillating tail fins in which motion of the tail region is thought to be the main source of thrust. This leads to the hypothesis that there may be homogeneity of muscle function and mechanical properties along the length of the body axis of anguilliform swimmers such as the eel (Wardle et al., 1995; D'Août and Aerts, 1999). To test this suggestion and to determine whether changes in muscle power output occur prior to migration, we have used the work loop technique (Josephson, 1985) to determine the net power output of the slow muscle of yellow- and silver-phase European eels. Muscle preparations were exposed to the full range of strains experienced by superficial, slow fibres during forward swimming (D'Août and Aerts, 1999). Power outputs were measured using optimal stimuli and *in vivo* stimuli obtained for *Anguilla rostrata* (Gillis, 1998b).

Materials and methods

European eels (*Anguilla anguilla* L.) were obtained from commercial fishermen. The fish were caught using nets in the freshwater fenland drains of south Lincolnshire, UK. Differences in coloration between different life-history stages were apparent, but coloration was variable. For this reason yellow- and silver-phase eels were distinguished on the basis of an eye size index I (Table 1):

$$I = 100\ \frac{\pi(A + B)^2/4}{BL},$$

(Pankhurst, 1982), where A and B are the horizontal and vertical eye diameters, respectively, and BL is body length (measurements in mm).

The fish were held in 2 m diameter fibreglass tanks containing aerated, filtered fresh water. The water temperature was maintained at 14 °C. A 16 h:8 h light:dark photoperiod was maintained in the aquarium. The eels were fed a maintenance diet of freeze-dried bloodworm three times a week.

Table 1. *Morphological values for the eels used in the study*

	Yellow	Silver	*P*
Mass (g)	683±73 (10)	726±28 (9)	0.634
Length (mm)	734±45 (10)	728±26 (9)	0.992
Eye index	13.2±0.9 (10)	20.0±1.0 (9)	0.002

Values are means ± S.E.M. (*N*).

Variables were tested for significant differences between phases using a Student's *t*-test.

Eels were killed by decapitation, destruction of the brain and pithing of the spinal cord. Blocks of superficial skeletal muscle tissue were removed from the lateral line region. These were placed in Ringer's solution (composition in mmol l^{-1}: NaCl, 109; KCl, 2.7; $NaHCO_3$, 2.5; $CaCl_2$, 1.8; $MgCl_2$, 0.47; sodium pyruvate, 5.3; Hepes, 10; pH 7.4±0.05 at 14 °C) oxygenated with 100 % oxygen and cooled to 8 °C. The tissue blocks were pinned out, and any fast muscle fibres, fat and skin were rapidly removed by dissection. The Ringer's solution was replaced frequently during dissection. The resulting muscle preparations consisted of a bundle of slow muscle fibres approximately 0.3 mm^2 in cross-sectional area and 3–4 mm in length running between two collagenous myosepta. Preparations were attached directly to the hooks of a servo arm and force transducer (AE801, SensoNor, Horten, Norway) *via* the thick collagenous myosepta. The length of the preparation was increased until it was approximately 0.5 mm less than the interseptal distance measured in the fish, and it was then left to recover for 1 h. The preparation was bathed in recirculating, oxygenated Ringer's solution at 14 °C. The work loop apparatus and techniques were as described previously (e.g. Altringham and Johnston, 1990; Hammond et al., 1998).

A substantial twitch response could not be obtained from the preparations; the twitch:tetanus ratio was approximately 0.15. For this reason, a brief tetanus was used to determine the required stimulus amplitude and resting length to give maximum isometric force production. Stimulus amplitude (2 ms pulses) was adjusted to 120 % of that giving a maximal response. The fibre length was then increased in 0.2 mm increments using a micromanipulator until the preparation yielded a maximal tetanic response. This was taken as resting length (l_0) and corresponded closely to the resting fibre length in the fish when lying flat. The stimulus frequency yielding a maximum tetanic response (180 Hz with little variation between preparations) was determined and used for subsequent work loop experiments. A standard tetanus (125 ms duration) was used to compare the mechanical properties of fibres from different axial locations and different life-history stages.

Muscle preparations were subjected to sinusoidal length changes and stimulated phasically. *In vivo* strain patterns in swimming fish are approximately sinusoidal (see Gillis,

1998b; Hammond et al., 1998; Knower et al., 1999; Ellerby et al., 2000). *In vivo* stimulus variables were derived from Gillis (Gillis, 1998b). Stimulus variables are expressed in degrees relative to a 360 ° sinusoidal strain cycle in which the muscle is at resting length l_0 and lengthening at 0 °. The phase of stimulus onset was 58 ° at 0.45 *BL* and 31 ° at 0.75 *BL*, where *BL* is total body length. Total stimulus duration was 102 ° at 0.45 *BL* and 108 ° at 0.75 *BL*. These data were obtained from *Anguilla rostrata* not *A. anguilla*. These two Atlantic eel species cannot be unambiguously separated on the basis of morphology or enzyme electrophoresis (Williams and Koehn, 1984). Small differences in mitochondrial DNA sequences separate the two species (e.g. Avise et al., 1990), but the difference between *A. anguilla* and *A. rostrata* is only slightly greater than the variation displayed within *A. anguilla* (Bastrop et al., 2000). On the basis of this high degree of similarity, it seemed reasonable to use these variables to approximate the *in vivo* stimulus patterns of *A. anguilla*.

In vivo, eel superficial muscle is exposed to a wide range of strains at different swimming speeds. Using the approximated *in vivo* stimulus variables, power output was determined at a range of muscle strains (±3 to ±12.5 % l_0) encompassing the range calculated for *A. anguilla* superficial muscle during forward swimming (D'Août and Aerts, 1999).

To determine the optimal stimulus variables for maximising power output, the stimulus onset relative to the strain cycle and the stimulus duration as a fraction of the strain cycle were systematically changed until the maximum power output for a given cycle frequency was obtained. Determination of optimum stimulus variables was carried out a strain of ±5 % l_0.

The muscle preparations were subjected to experimental runs of five cycles. Work and power were calculated using the work loop technique (e.g. Josephson, 1985; Altringham and Johnston, 1990). Power output stabilised after the first cycle. Work and power output measurements were derived from the third cycle. Preparations were allowed to rest for 6 min between experimental runs to minimise fatigue. On completion of an experiment, the preparation was removed from the chamber. The preparation was viewed using a binocular microscope, and non-contractile cells were identified by applying an electrical stimulus. The connective tissue of the myosepta and the dead cells were cut away. The remaining tissue was blotted to remove excess Ringer's solution prior to weighing. Cross-sectional area was calculated as volume/length of the preparation, where volume was determined assuming a value for muscle density of 1060 kg m^{-3}.

To detect any change in muscle performance during the experiment, preparations were subjected to a control trial, with fixed variables (cycle frequency 0.5 Hz, strain 5 % l_0, stimulus onset/duty cycle 50 °/100 °) after every fourth run. Power outputs were scaled relative to these control trials. After an increase in power output during the initial stages of the trial, power output stabilised and remained virtually constant for the remainder of the experiment (up to 6 h in total).

Kinematic analysis

To generate a range of swimming speeds and tailbeat frequencies, kinematic data were obtained in a flow tank. The working cross section of the tank was 25 cm×21 cm. Fish were exposed to a range of length-specific flow velocities from 0.25 to 0.7 *BL* s^{-1} (where *BL* is body length). Experiments were recorded using a Canon EX2 Hi-8 video camera mounted above the tank. An ATI All-in Wonder Pro video card and software were used to grab video frames for kinematic analysis. Frames were grabbed at a resolution of 640×480 pixels. This meant that measurements could be made to an accuracy of approximately 2 mm. The frame rate of 50 Hz gave a time resolution of 0.02 s. Measurements were made from still frames using Sigma Scan Pro image-analysis software. Cartesian coordinates were recorded at six points along the length of the fish. These were the snout, 0.2, 0.4, 0.6 and 0.8 *BL* and the tip of the tail. The displacements of these points through time were used to calculate tailbeat frequency and maximum lateral displacement at a given point. Swimming sequences in which the fish was within 5 cm of the wall were excluded from the analysis.

Statistical analyses

Statistical analyses were carried out using SigmaStat (SPSS, Chicago, IL, USA) software. Basic muscle mechanical properties and optimal stimulus variables were tested for significant differences between body positions and life-history stages using analysis of variance (ANOVA). Significant differences were measured using the Student–Newman–Keuls test. Values are shown as means ± S.E.M.

Results

Slow muscle isometric properties

Maximum isometric tetanic stress did not change significantly with body position in the yellow- (q=2.9, P>0.05, Student–Newman–Keuls) or silver-phase eel (q=2.1, P>0.05, Student–Newman–Keuls). Maximum isometric tetanic stress was significantly higher in the silver- than in the yellow-phase eel (q=12.3, P<0.05, Student–Newman–Keuls). The time to peak force T_a did not differ significantly with body position (two-way ANOVA, P=0.574) or life-history phase (two-way ANOVA, P=0.052). Time from stimulus offset to 90 % relaxation T_{90} showed significant differences between life-history stages (two-way ANOVA, P<0.001) and between body positions (two-way ANOVA, P=0.029). T_{90} was significantly greater in yellow- than in silver-phase eels (q=11.1, P<0.05, Student–Newman–Keuls). In yellow-phase eels, there was no significant difference in T_{90} with body position (P=0.860, Student–Newman–Keuls), but in silver-phase eels T_{90} was significantly longer in the posterior muscle (q=4.7, P<0.05, Student–Newman–Keuls). The mechanical properties of slow-twitch muscle are summarised in Table 2.

Slow muscle power output

The onset and duration of stimuli were systematically

Table 2. *Summary of the mechanical properties of yellow- and silver-phase eel slow muscle*

	Yellow		Silver	
	0.45 *BL*	0.75 *BL*	0.45 *BL*	0.75 *BL*
Maximum isometric stress (kN m^{-2})	65.2±1.8^{a} (5)	78.1±4.7^{a} (5)	115.6±5.4^{b} (5)	106.2±5.1^{b} (5)
Time to peak force, T_a (ms)	82±1.2^{c} (5)	83±1.2^{c} (5)	77±0.7^{c} (5)	84±1.5^{c} (5)
Time from stimulus offset to 90 % relaxation, T_{90} (ms)	480±6^{d} (5)	472±6^{d} (5)	402±7^{e} (5)	437±12^{f} (5)
Peak power output (W kg^{-1}) at a strain ±5 % l_0 using an optimal stimulus	0.22±0.04^{g} (5)	0.43±0.09^{h} (4)	1.29±0.05^{i} (4)	1.12±0.05^{i} (4)
Peak power output (W kg^{-1}) at a strain ±5 % l_0 using approximated *in vivo* stimuli	0.05±0.05^{j} (5)	0.18±0.06^{j} (4)	0.74±0.09^{k} (4)	0.67±0.06^{k} (4)

T_a and T_{90} were measured on the basis of a 125 ms, 180 Hz tetanic stimulus with a 2 ms pulse duration. Power outputs were obtained at a cycle frequency of 0.5 Hz.

Values marked with the same letter are not significantly different (P>0.05, Student–Newman–Keuls).

Values are means ± S.E.M. (N).

BL, body length; l_0, optimum length.

changed to find the stimulus variables that maximised power output. At a cycle frequency of 0.5 Hz, maximum power output using optimal stimulus variables did not differ significantly with body position in the silver-phase eel (q=0.5, P>0.05, Student–Newman–Keuls). In yellow-phase eels under optimal stimulus conditions, the power output of the posterior muscle was significantly greater than that of the anterior muscle (q=3.8, P<0.05, Student–Newman–Keuls). Maximum power output was significantly greater in silver- than in yellow-phase slow muscle (two-way ANOVA, P<0.001) (Table 2). Power outputs peaked at cycle frequencies of 0.5–0.8 Hz in silver-phase muscle and 0.3–0.5 Hz in yellow-phase muscle (Fig. 1).

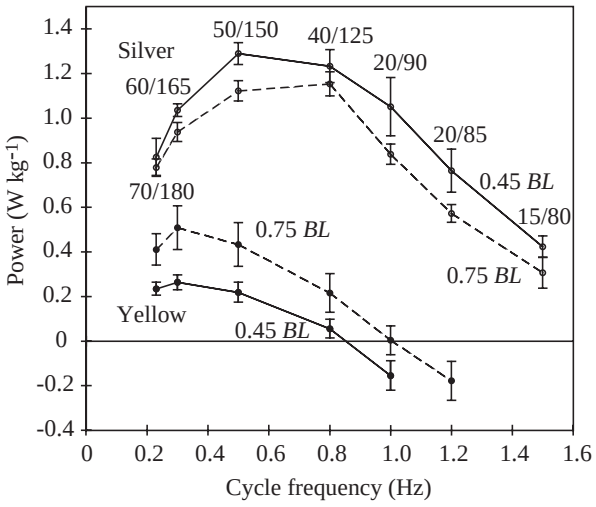

Fig. 1. Optimal power outputs of yellow- and silver-phase eel slow muscle *versus* cycle frequency. Optimal stimulus variables are shown as onset phase/duration (both in degrees). Optimal stimulus variables apply to both life-history stages. Open symbols represent silver-phase eel slow muscle and filled symbols represent yellow-phase eel slow muscle. Data from 0.45 *BL*, where *BL* is body length, are joined by solid lines, and data from 0.75 *BL* are joined by dashed lines. Values are means ± S.E.M.; N=5 for yellow eel at 0.45 *BL*, N=4 for all other data sets.

At a cycle frequency of 0.5 Hz, maximum power output using *in vivo* stimulus variables did not differ significantly with body position in the yellow- or silver-phase eels (two-way ANOVA, P=0.576). At this cycle frequency, maximum power output using *in vivo* stimulus variables was significantly greater in silver- than in yellow-phase eels (two-way ANOVA, P<0.001, q=12.6, P<0.05, Student–Newman–Keuls). Power outputs obtained using approximated *in vivo* stimuli were lower than those obtained using optimal stimuli (Fig. 2; Table 2).

Optimal stimulus conditions for power output

Overall, the optimal stimulus onset was not significantly different between life-history phases (three-way ANOVA, P=0.096) or body positions (three-way ANOVA, P=0.826). There was a significant change in optimal onset with cycle frequency (three-way ANOVA, P<0.001). Optimal stimulus onsets tended to be earlier at higher cycle frequencies.

There was no significant difference in optimal duty cycle between life-history phases (three-way ANOVA, P=0.074) or between body positions (three-way ANOVA, P=0.264). There was a significant change in optimal duty cycle with cycle frequency (three-way ANOVA, P<0.001). Optimal duty cycles tended to be shorter at higher cycle frequencies. The mean onset/duty cycles for maximum power output are shown in Fig. 1.

Muscle strain and power output

The response of slow muscle to increasing strain amplitudes was dependent on cycle frequency. At 0.3 Hz, silver-phase slow muscle showed an increase in power production with increasing strain from ±3 to ±10 % l_0 (Fig. 3A). Above strains of ±10 % l_0, power production

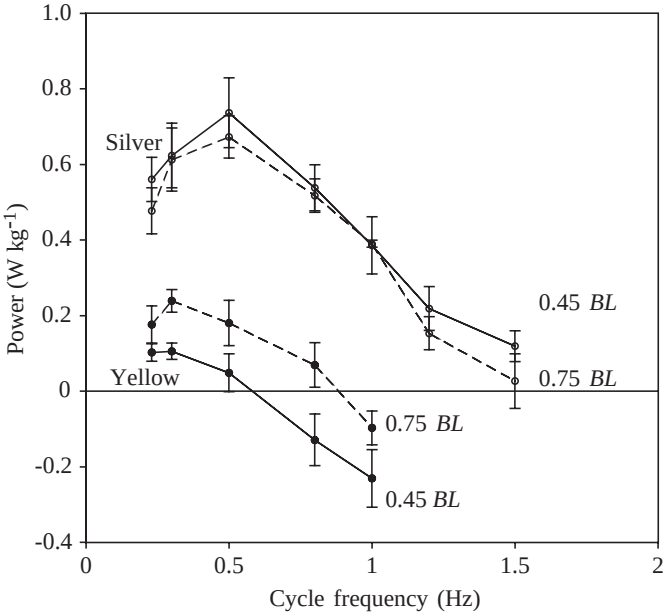

Fig. 2. Power outputs of yellow- and silver-phase eel slow muscle *versus* cycle frequency using approximate *in vivo* stimulus variables. Stimulus variables were obtained from Gillis (1998b). Open symbols represent silver-phase eel slow muscle and filled symbols represent yellow-phase eel slow muscle. Data from 0.45 *BL*, where *BL* is body length, are joined by solid lines, and data from 0.75 *BL* are joined by dashed lines. Values are means ± S.E.M.; *N*=5 for yellow eel at 0.45 *BL*, *N*=4 for all other data sets.

tended to level off. This was also the case in yellow-phase slow muscle from 0.75 *BL*. In yellow-phase eel slow muscle from 0.45 *BL*, power output declined at strains above ±5 % l_0. At 0.5 Hz, the pattern remained similar in silver eel slow muscle from 0.45 *BL* (Fig. 3B). However, in slow muscle from both silver- and yellow-phase eels at 0.75 *BL*, there was a decline in power production above strains of ±10 % l_0 at this cycle frequency. Yellow-phase slow muscle from 0.45 *BL* could no longer achieve positive power output above strains of ±5 % l_0 at this frequency. At 0.8 Hz, there was no positive power output by yellow-phase slow muscle from 0.45 *BL*, and these data have been omitted from Fig. 3C. Yellow-phase slow muscle from 0.75 *BL* could not produce positive power above strains of ±7.5 % l_0 at 0.8 Hz (Fig. 3C). In silver-phase slow muscle from both positions, power output peaked at strains of ±5 to ±7.5 % l_0.

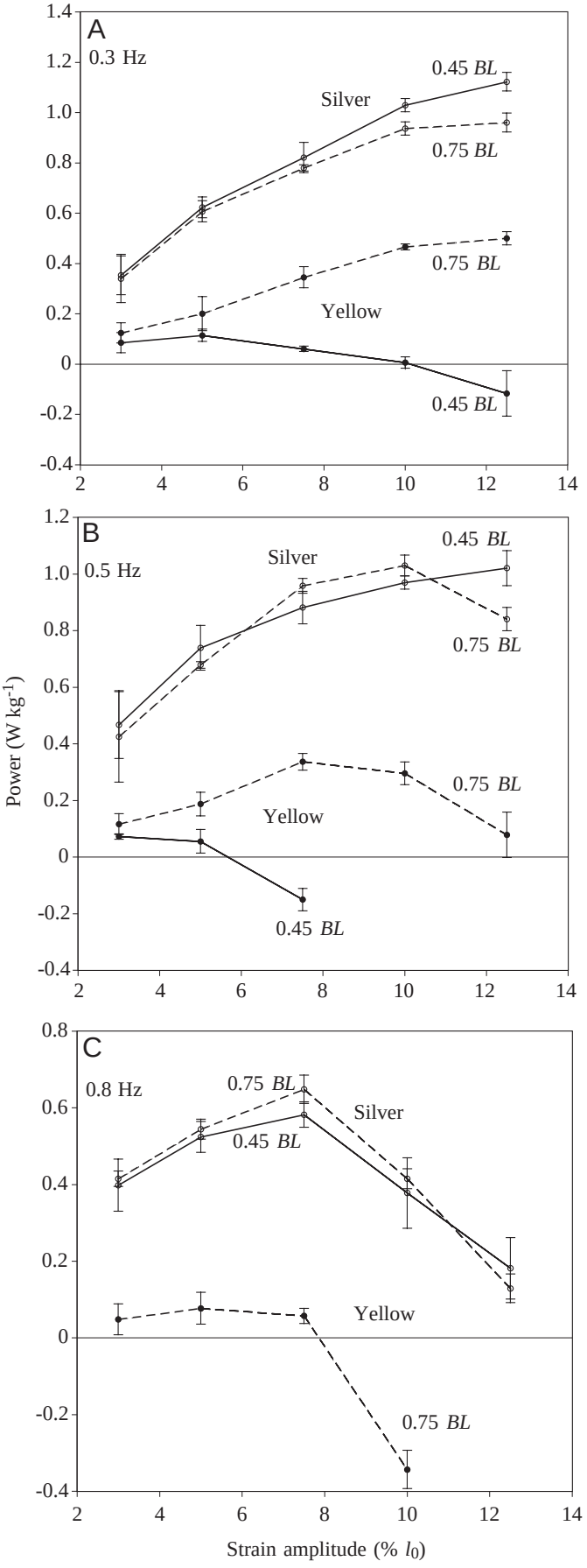

Fig. 3. Power output *versus* muscle strain for yellow- and silver-phase eel slow muscle. (A) Cycle frequency 0.3 Hz; (B) cycle frequency 0.5 Hz; (C) cycle frequency 0.8 Hz. Open symbols represent silver-phase eel slow muscle and filled symbols represent yellow-phase eel slow muscle. Data from 0.45 *BL*, where *BL* is body length, are joined by solid lines, and data from 0.75 *BL* are joined by dashed lines. Strain is the percentage length change of the preparation ±l_0, where l_0 is the length of preparation that yields maximum isometric stress. Values are means ± S.E.M.; *N*=5 for yellow eel at 0.45 *BL*, *N*=4 for all other data sets.

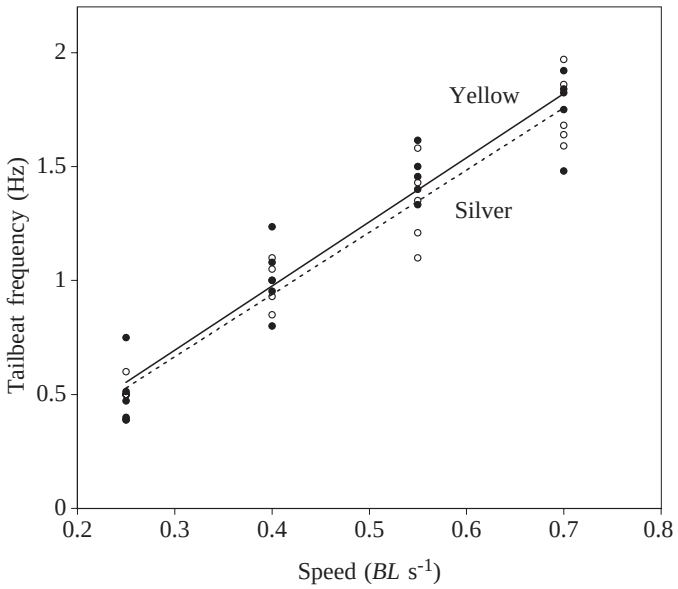

Fig. 4. Tailbeat frequency as a function of length-specific swimming speed of yellow- and silver-phase eels. Filled data points represent yellow-phase eels and open data points represent silver-phase eels. Data are fitted with linear regression lines. The solid line is fitted to the data points for yellow-phase eels, the dashed line is fitted to the data points for silver-phase eels. Equations are given in the text. Values are means ± S.E.M. (N=5). *BL*, body length.

Kinematics

Tailbeat frequency showed a linear relationship with swimming speed in both yellow- and silver-phase eels (Fig. 4). In yellow-phase eels, tailbeat frequency (f) was related to length-specific speed (U_{sp}) by the equation $f=2.82U_{sp}-0.15$ (r^2=0.92, P<0.01, Pearson correlation). In silver-phase eels, the corresponding equation was $f=2.73U_{sp}-0.16$ (r^2=0.93, P<0.01, Pearson correlation). At a swimming speed of $0.25\,BL\,s^{-1}$, there was no apparent difference in the degree of lateral displacement of the body between yellow- and silver-phase eels (Fig. 5A). In both life-history stages, lateral movement was confined largely to the posterior half of the body. At a swimming speed of $0.4\,BL\,s^{-1}$, a difference in swimming kinematics emerged (Fig. 5B). In the silver-phase eel, lateral displacement was still largely confined to the posterior half of the body, whilst in the yellow-phase eel there was now a greater degree of lateral displacement in the anterior part of the body. At a speed of $0.55\,BL\,s^{-1}$, swimming kinematics again became similar in terms of lateral displacement. The anterior part of the body underwent greater lateral displacement in both life-history stages than at lower swimming speeds.

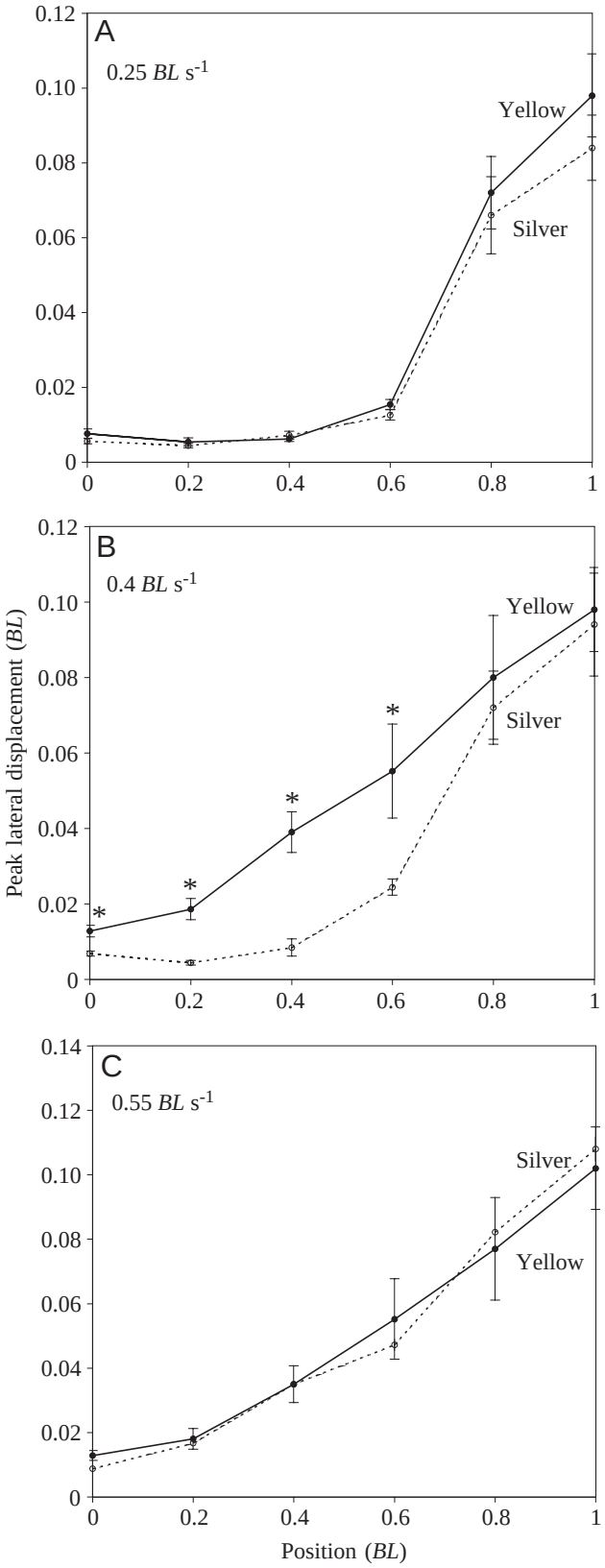

Fig. 5. Peak lateral displacement of the body during swimming of yellow- and silver-phase eels. Filled data points and solid lines represent yellow-phase eels, open data points and dashed lines represent silver-phase eels. Position 0 *BL*, where *BL* is body length, is the tip of the snout and 1.0 *BL* is the tail tip. (A) Swimming speed $0.25\,BL\,s^{-1}$. (B) Swimming speed $0.40\,BL\,s^{-1}$. (C) Swimming speed $0.55\,BL\,s^{-1}$. Values are means ± S.E.M. (N=5). Values marked with an asterisk are significantly different between the two life-history phases (Student's t-test, P<0.05).

Discussion

Slow muscle isometric properties

The isometric properties of yellow-phase slow muscle did not change with axial location. In silver-phase eels, the isometric properties were also uniform, except for the post-tetanic relaxation times, which showed a small but significant increase in the posterior muscle. This fits the pattern observed in the slow (e.g. Swank et al., 1997; Coughlin, 2000) and fast (e.g. Altringham et al., 1993; Davies et al., 1995) muscle of some other teleost species. However, the change in properties was small relative to these other species. Overall, the isometric muscle properties support the hypothesised uniformity of muscle properties in an anguilliform swimmer.

The isometric stresses measured in yellow-phase slow muscle (65–78 kN m^{-2}) appear low relative to those measured in some other teleosts. Isometric stresses based on myofibrillar area ranged from 110 to 160 kN m^{-2} in the scup (*Stenotomus chrysops*; Rome et al., 2000), in which myofibrillar area is only 43 % of the total muscle tissue cross-sectional area. The stresses measured in the present study were based on total tissue area. If the stresses measured in scup are converted to tissue area stresses, then they range from 47 to 69 kN m^{-2}. Under isometric conditions, the ability of yellow-phase slow muscle to exert stresses is similar to that of scup slow muscle, whilst silver-phase slow muscle can exert greater stresses. Directly comparable slow muscle tissue stresses have been measured (Hammond et al., 1998) in rainbow trout (*Oncorhynchus mykiss*). These ranged from 132 to 140 kN m^{-2}, approximately twice the isometric stress measured in yellow-phase slow muscle in the present study. Myofibrillar stresses measured in the rainbow trout and largemouth bass (*Micropterus salmoides*) were higher (170 and 186 kN m^{-2} respectively; Coughlin, 2000). The variation in myofibrillar properties appears to be smaller than the variation in muscle tissue properties. Most of the existing data on the amounts of muscle tissue in teleost fish are expressed in terms of muscle tissue mass or volume, not in terms of myofibrillar mass or volume. When considering how whole-organism locomotory performance is dictated by muscle properties, it is important that the level of performance of the muscle tissue as a whole, not just its contractile component, is understood.

Slow muscle power output

The differences in slow muscle power output between yellow- and silver-phase eel are striking (Table 2; Figs 1, 2). In the American eel, the relative proportion of slow muscle increased from 8.6 to 14.4 % of the total muscle mass in the transition from the yellow to the silver phase (Eggington, 1986). This means that not only does the mass-specific power output of slow muscle increase during metamorphosis, but that the overall potential power output of silver-phase eels is increased by this growth in muscle mass. If a similar increase in muscle mass were to occur in the European eel, total slow muscle power output would be almost seven times greater in silver- than in yellow-phase eels (on the basis of an average maximum power output using approximated *in vivo* stimuli). The ability of silver-phase slow muscle to generate more work per cycle, and therefore more power, than yellow-phase slow muscle may be due to its ability to exert larger stresses (Table 2).

Power outputs obtained using optimal stimuli are approximately twice as high as those obtained using approximated *in vivo* stimuli (Figs 1, 2; Table 2). This is because the *in vivo* stimulus variables from *A. rostrata* did not match those required for maximum power output at any of the cycle frequencies at which power measurements were obtained. Despite their close phylogenetic affinities, the American and European eel may have different patterns of muscle activation. However, maximising power output is not necessarily the main consideration *in vivo*. In dogfish (*Scyliorhinus canicula*) slow muscle, the operating conditions for obtaining maximum efficiency are different from those required for obtaining maximum power output (Curtin and Woledge, 1993). It may be the case that during a lengthy migration efficiency is more important than maximising power output.

The mass-specific power outputs measured in this study (up to 1.3 W kg^{-1}) appear low in comparison with the values obtained for slow muscle from other fish. Mass-specific power outputs measured in scup slow muscle under approximated *in vivo* conditions ranged from 4.39 W kg^{-1} anteriorly to 24.32 W kg^{-1} posteriorly (Rome et al., 1993). These power outputs were obtained at a cycle frequency of 6.4 Hz, much higher than the maximum cycle frequency attained by eel slow muscle. Because of the large differences in cycle frequency range, the work output per cycle provides a better means for comparing muscle performance. At maximum power output under '*in vivo*' conditions, the work production per cycle ranged from 0.37 to 0.80 J kg^{-1} in yellow-phase slow muscle and 1.34–1.48 J kg^{-1} in silver-phase slow muscle. These compare with '*in vivo*' work production values ranging from 0.68 to 3.80 J kg^{-1} in the scup (Rome et al., 1993). The latter measurements were based on estimated myofibrillar masses that were only 43 % of the total tissue mass (Rome et al., 1992). The remainder of the preparation consisted of connective tissue and fat cells. The measurements of eel muscle power output were based on total tissue mass rather than estimated myofibrillar mass. To make the values directly comparable, the work outputs for scup need to be scaled down accordingly, yielding values of 0.29–1.63 J kg^{-1}. In terms of work output, eel slow muscle is comparable with other teleost slow muscle.

The only previous power measurement obtained for eel muscle was from the American eel *Anguilla rostrata* (Long, 1998). The maximum power output was 23 W kg^{-1}, much greater than in the present study. This measurement was obtained using whole-body work loops. Experimental conditions were intended to mimic steady swimming conditions; however, they were conducted at a cycle frequency of 3 Hz and involved stimulating the entire lateral musculature. It seems unlikely that this tailbeat frequency could be sustained *in vivo*. The conditions were those of a fast start or unsustained burst rather than those that would be encountered during steady

swimming. The majority of the myotomal muscle is made up of fast fibres, so this was essentially a measure of fast muscle power output.

A major determinant of power output is the cycle frequency at which the muscle operates. The maximum cycle frequencies at which eel slow muscle can produce positive power and the optimal frequencies for maximum power production are much lower than those that can be achieved by slow muscle from other fish. Scup slow muscle was able to produce positive power at a cycle frequency of 6.4 Hz (Rome et al., 1993), and rainbow trout slow muscle was capable of producing positive power at cycle frequencies of up to 5 Hz, with power output peaking at 2–3 Hz (Hammond et al., 1998). Direct comparison is difficult because of the different temperatures at which the experiments were conducted (present study 14 °C; trout 9 °C; scup, not stated). The inability of eel slow muscle to produce positive power at high frequencies may be related to long relaxation times (Table 2). Post-tetanic relaxation times measured in the scup (146 ms anteriorly increasing to 271 ms posteriorly; Swank et al., 1997) were shorter than those in the eel (402–480 ms; Table 2). Long relaxation times tend to limit power production at higher cycle frequencies by preventing the muscle from relaxing fully before the subsequent stimulus. The significantly shorter T_{90} values obtained for silver-phase slow muscle may account for the ability of silver-phase slow muscle to produce net positive power at higher cycle frequencies than yellow-phase slow muscle. No difference in peak frequency was apparent between anterior and posterior muscle in silver-phase eels despite differences in T_{90}. Any difference in the frequency response may have been obscured by the variability in the data sets.

Under approximated *in vivo* conditions, there was no significant change in mass-specific muscle power output with axial location. This was also the case in silver-phase slow muscle under optimal stimulus conditions for maximum power output. However, in yellow-phase slow muscle with an optimal stimulus, the posterior muscle generated a greater mass-specific power output than the anterior muscle. The underlying reasons for higher power output in yellow-phase posterior muscle relative to anterior muscle are not immediately clear. There are no significant differences in isometric properties with axial location. Isometric stress was higher in the posterior muscle, but not significantly so. Axial patterns of power production are determined by muscle distribution as well as by muscle properties and activation patterns. The axial distribution of eel slow muscle is fairly uniform relative to that of other teleosts, in which there is usually a clear peak in slow muscle area at approximately 0.5 *BL* in scombrids or at 0.6–0.7 *BL* in non-scombrids (Ellerby et al., 2000). Overall, the data suggest uniformity of axial power production in anguilliform swimmers relative to fish in which the caudal fin is the main source of thrust.

Muscle strain

D'Août and Aerts (D'Août and Aerts, 1999) calculated superficial slow muscle strains at a speed of 0.48 $BL\,s^{-1}$ of approximately ±5 % at 0.45 *BL*, increasing to ±8 % at 0.75 *BL*. This swimming speed would require a tailbeat frequency of approximately 1.2 Hz. Yellow-phase slow muscle would not be able to sustain positive power output at this tailbeat frequency and strain (Fig. 3B,C). At the highest frequency at which slow muscle was exposed to a range of strains (0.8 Hz), some positive power could be produced by the posterior slow muscle at a strain of ±7.5 % (Fig. 3C). At a speed of 0.841 $BL\,s^{-1}$ (tailbeat frequency 2.7 Hz), superficial muscle strain increased to ±12 % at 0.45 *BL* and ±10 % at 0.75 *BL* (D'Août and Aerts, 1999). At this higher speed, with higher tailbeat frequencies, yellow-phase slow muscle cannot produce positive power at these strains. Fast muscle fibres must power these higher tailbeat frequencies because fast fibres closer to the backbone undergo lower strains (Alexander, 1969) and have faster shortening velocities (Rome et al., 1988). During backwards swimming, superficial muscle strains approached ±25 % l_0. It seems unlikely that slow muscle can contribute much positive power output during backwards swimming.

Swimming performance

The characteristics of eel slow muscle suggest a low level of sustainable swimming performance in terms of tailbeat frequency and swimming speed relative to other teleosts. Also, yellow-phase eels should have a lower maximum sustainable swimming speed and tailbeat frequency than silver-phase eels.

Gillis (Gillis, 1998b) found that the slow muscle was consistently active across the range of speeds examined (0.5–1.0 $BL\,s^{-1}$). This corresponds to an approximate tailbeat frequency range of 1.6–2.7 Hz. It is clear that the properties of eel slow muscle measured in the present study mean that it could not power swimming at these cycle frequencies. There are two possible explanations for this apparent mismatch of *in vivo* and *in vitro* performance. Gillis (Gillis, 1998b) measured swimming performance and muscle activity at 19.5 °C. The present *in vivo* experiments were conducted at 14 °C. In yellowfin tuna (*Thunnus albacares*) and Pacific bonito (*Sarda chiliensis*), a rise in temperature from 15 to 20 °C resulted in a doubling of the cycle frequency at which peak power production was achieved (Altringham and Block, 1997). A similar effect in the eel would have allowed the slow muscle to operate at higher cycle frequencies than in the present study. Also, fast muscle was recruited in addition to slow muscle and was active during 20 % of tailbeat cycles at a speed of 0.75 $BL\,s^{-1}$ (Gillis, 1998b). This intermittent recruitment pattern suggests that as tailbeat frequency increased above approximately 2 Hz American eels were incapable of maintaining a steady swimming velocity using slow muscle alone. This is much lower than the tailbeat frequencies that can be maintained using slow muscle alone in other teleosts (e.g. Johnston et al., 1977; Jayne and Lauder, 1994). If the temperature difference and additional recruitment of fast muscle are taken into account, then the differences between *in vivo* and *in vitro* performance are small.

Mean tailbeat frequencies can obscure differences in kinematics and the underlying patterns of muscle activity. At

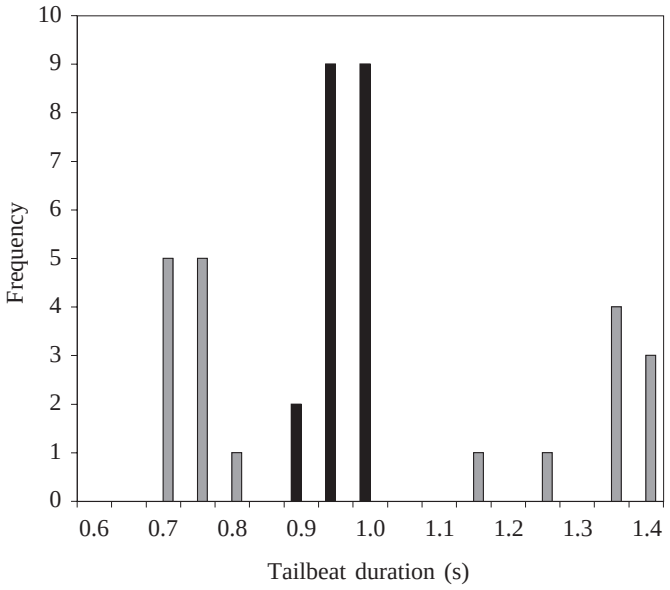

Fig. 6. Frequency distribution of tailbeat duration in yellow- and silver-phase eels swimming at 0.40 *BL* s^{-1}, where *BL* is body length, from typical swimming sequences. The data represent 20 consecutive tailbeat periods. Black columns represent silver-phase eel and grey columns represent yellow-phase eel.

a swimming speed of 0.4 *BL* s^{-1}, mean tailbeat frequencies were similar in yellow- and silver-phase eels, both being approximately 1.0 Hz (Fig. 4). However, the frequency distribution of tailbeat durations within a sequence of 20 tailbeats showed differences between the two life-history phases. In silver-phase eels, tailbeat duration was relatively constant, but in yellow-phase eels the distribution of tailbeat durations was bimodal (Fig. 6). Periods of low-tailbeat-frequency swimming were interspersed by short bursts of higher-tailbeat-frequency swimming. The slow muscle properties measured *in vivo* would make it unsuitable for producing positive power during these bursts. This suggests that yellow-phase eels are using unsustained bursts of fast muscle activity to maintain a swimming speed that silver-phase eels can maintain using sustained muscle activity.

Some data exist from tagging studies that give an indication of movements and swimming performance in the wild during both life-history stages of anguillid eels. Estimates of home range size in yellow-phase eels are generally small (<100 m^2, Ford and Mercer, 1986; 1300–2700 m^2, Labar et al., 1987). Mean speeds of yellow-phase American eels ranged from 0.0014 to 0.38 *BL* s^{-1} (Parker, 1995). These displaced eels moved with tidal flows in 94 % of cases. The combination of a small home range, low speeds and a reliance on favourable currents during homing suggests that the locomotory performance of the yellow-phase eel is relatively poor. The swimming speeds of silver *A. anguilla* in the open North Atlantic have yet to be measured. Migrating Japanese silver-phase eels (*Anguilla japonica*) have been tracked in the open ocean at a mean speed of 0.48 *BL* s^{-1} (Aoyama et al., 1999). Assuming that migrating European silver eel achieve a similar speed, this would require a tailbeat frequency of approximately 1.2 Hz, yielding a speed of 0.29 m s^{-1} in a 60 cm eel (assuming a stride length of 0.4 *BL*; Gillis, 1998a). The distance from the UK to the Sargasso Sea is approximately 5000 km. At a speed of 0.29 m s^{-1}, the journey would take 28.5 weeks. Eels commence their spawning migration in late summer or autumn (Lowe, 1952; Vøllestad et al., 1986; Poole et al., 1990). Assuming a September departure, this would result in arrival at the spawning grounds in March/April, which is when spawning is believed to occur (McCleave et al., 1987). Whilst positive power is produced by silver-phase slow muscle at a cycle frequency of 1.2 Hz, power output is much lower than the peak power output (0.22 W kg^{-1} compared with 0.74 W kg^{-1} in the anterior muscle). This suggests that silver-phase eels may have difficulty achieving this speed using slow muscle alone. Intermittent recruitment of fast muscle to increase overall swimming speed is a possibility, as is the use of favourable currents, as exploited by silver-phase eels in the North Sea (McCleave and Arnold, 1999). The silver-phase eels used in this study were captured several months prior to their autumn migration, so further improvement in the locomotory performance of slow muscle may occur in the months preceding their departure.

D.J.E. was supported by a BBSRC special studentship. I.L.Y.S. was supported by a grant from the Niels Stensen Foundation.

References

Alexander, R. McN. (1969). The orientation of muscle fibres in the myomeres of fish. *J. Mar. Biol. Ass. U.K.* **49**, 263–290.

Altringham, J. D. and Block, B. A. (1997). Why do tuna maintain elevated slow muscle temperatures: power output of muscle isolated from endothermic and ectothermic fish. *J. Exp. Biol.* **200**, 2617–2627.

Altringham, J. D. and Ellerby, D. J. (1999). Fish swimming: patterns in muscle function. *J. Exp. Biol.* **202**, 3397–3403.

Altringham, J. D. and Johnston, I. A. (1990). Scaling effects in muscle function: power output of isolated fish muscle fibres performing oscillatory work. *J. Exp. Biol.* **148**, 395–402.

Altringham, J. D., Wardle, C. S. and Smith, C. I. (1993). Myotomal muscle function at different locations in the body of a swimming fish. *J. Exp. Biol.* **182**, 191–206.

Aoyama, J., Hissmann, K., Yoshinga, T., Sasai, S., Uto, T. and Ueda, H. (1999). Swimming depth of migrating silver eels *Anguilla japonica* released at seamounts off the West Mariana Ridge, their estimated spawning sites. *Mar. Ecol. Prog. Ser.* **186**, 265–269.

Avise, J. C., Nelson, W. S., Arnold, J., Koehn, R. K., Williams, G. C. and Thorsteinsson, V. (1990). The evolutionary genetic status of Icelandic eels. *Evolution* **44**, 1254–1262.

Bastrop, R., Strehlow, B., Jürss, K. and Sturmbauer, C. (2000). A new molecular phylogenetic hypothesis for the evolution of freshwater eels. *Mol. Phylogenet. Evol.* **14**, 250–258.

Bone, Q. (1966). On the function of the two types of myotomal muscle fibre in elasmobranch fish. *J. Mar. Biol. Ass. U.K.* **46**, 321–349.

Breder, C. M. (1926). The locomotion of fishes. *Zoologica* **4**, 159–297.

Colombo, G. and Rossi, R. (1978). Environmental influences on growth and sex ratio in different eel populations (*Anguilla anguilla* L.) of Adriatic coasts. In *Physiology and Behaviour of Marine Organisms* (ed. D. S. McClusky and A. J. Berry), pp. 313–320. Oxford: Pergamon Press.

Coughlin, D. J. (2000). Power production during steady swimming in largemouth bass and rainbow trout. *J. Exp. Biol.* **203**, 617–629.

Coughlin, D. J. and Rome, L. C. (1999). Muscle activity in steady swimming scup, *Stenotomus chrysops*, varies with fiber type and body position. *Biophys. J.* **196**, 145–152.

Curtin, N. A. and Woledge, R. C. (1993). Efficiency of energy conversion during sinusoidal movement of red muscle fibres from the dogfish *Scyliorhinus canalicula*. *J. Exp. Biol.* **185**, 195–206.

Curtin, N. A. and Woledge, R. C. (1996). Power at the expense of efficiency in the contraction of white muscle from dogfish *Scyliorhinus canicula*. *J. Exp. Biol*. **199**, 593–601.

D'Août, K. and Aerts, P. (1999). A kinematic comparison of forward and backward swimming in the eel *Anguilla anguilla*. *J. Exp. Biol.* **202**, 1511–1521.

Davies, M. L. F., Johnston, I. A. and Vandewal, J. (1995). Muscle-fibers in rostral and caudal myotomes of the Atlantic cod (*Gadus morhua*, L.) have different mechanical properties. *Physiol. Zool*. **68**, 673–697.

Deelder, C. L. (1958). On the behaviour of elvers (*Anguilla vulgaris* Turt.) migrating from the sea into fresh water. *J. Conseil Permanent Int. l'Expl. Mer* **24**, 135–146.

Eggington, S. (1986). Metamorphosis of the American eel, *Anguilla rostrata* LeSeur. II. Structural reorganisation of the locomotory musculature. *J. Exp. Zool.* **238**, 297–309.

Ellerby, D. J., Altringham, J. D., Williams, T. and Block, B. A. (2000). Slow muscle function of Pacific bonito (*Sarda chiliensis*) during steady swimming. *J. Exp. Biol*. **203**, 2001–2013.

Ford, T. E. and Mercer, E. (1986). Density, size distribution and home range of American eels, *Anguilla rostrata*, in a Massachusetts salt marsh. *Env. Biol. Fish*. **17**, 309–314.

Frolich, L. M. and Biewener, A. A. (1992). Kinematic and electromyographic analysis of the functional role of the body axis during terrestrial and aquatic locomotion in the salamander *Ambystoma tigrinum. J. Exp. Biol*. **162**, 107–130.

Gillis, G. B. (1996). Undulatory locomotion in elongate aquatic vertebrates: anguilliform swimming since Sir James Gray. *Am. Zool*. **36**, 656–665.

Gillis, G. B. (1998a). Environmental effects on undulatory locomotion in the American eel *Anguilla rostrata*: kinematics in water and on land. *J. Exp. Biol*. **201**, 949–961.

Gillis, G. B. (1998b). Neuromuscular control of anguilliform locomotion: patterns of red and white muscle activity during swimming in the American eel *Anguilla rostrata*. *J. Exp. Biol*. **201**, 3245–3256.

Gillis, G. B. (2000). Patterns of white muscle activity during terrestrial locomotion in the American eel (*Anguilla rostrata*). *J. Exp. Biol*. **203**, 471–480.

Graham, J. B., Lowell, W. R., Rubinoff, I. and Motta, J. (1987). Surface and subsurface swimming of the sea snake *Pelamis platurus. J. Exp. Biol*. **127**, 27–44.

Gray, J. (1933). Studies in animal locomotion. I. The movement of fish with special reference to the eel. *J. Exp. Biol*. **10**, 88–104.

Grillner, S. and Kashin, S. (1976). On the generation and performance of swimming in fish. In *Neural Control of Locomotion* (ed. R. M. Herman, S. Grillner, P. S. G. Stein and D. G. Stuart), pp. 181–201. New York: Plenum.

Hammond, L., Altringham, J. D. and Wardle, C. S. (1998). Myotomal slow muscle function of rainbow trout *Oncorhynchus mykiss* during steady swimming. *J. Exp. Biol.* **201**, 1659–1671.

Jayne, B. C. (1988). Muscular mechanisms of snake locomotion: an electromyographic study of lateral undulation of the Florida Banded Water Snake (*Nerodia fasciata*) and the Yellow Rat Snake (*Elaphe obsoleta*). *J. Morph.* **197**, 159–181.

Jayne, B. C. and Lauder, G. V. (1994). How swimming fish use slow and fast muscle fibres: implications for models of vertebrate muscle recruitment. *J. Comp. Physiol.* A **175**, 123–131.

Jayne, B. C. and Lauder, G. V. (1995). Are muscle fibers within fish myotomes activated synchronously? Patterns of recruitment within deep myomeric musculature during swimming in largemouth bass. *J. Exp. Biol*. **198**, 805–815.

Johnson, T. P., Syme, D. A., Jayne, B. C., Lauder, G. V. and Bennett, A. F. (1994). Modeling red muscle power output during steady and unsteady swimming in largemouth bass. *Am. J. Physiol*. **267**, 418–488.

Johnston, I. A., Davison, W. and Goldspink, G. (1977). Energy metabolism of carp swimming muscles. *J. Comp. Physiol.* **114**, 203–216.

Josephson, R. K. (1985). Mechanical power output from striated muscle during cyclic contractions. *J. Exp. Biol.* **114**, 493–512.

Knower, T., Shadwick, R. E., Katz, S. L., Graham, J. B. and Wardle, C. S. (1999). Red muscle activation patterns in yellowfin (*Thunnus albacares*) and skipjack (*Katsuwonus pelamis*) tunas during steady swimming. *J. Exp. Biol.* **202**, 2127–2138.

Labar, G. W., Casal, J. A. and Delgado, C. F. (1987). Local movements and population size of European eels (*Anguilla angu*illa) in a small lake in south-western Spain. *Env. Biol. Fish*. **19**, 111–117.

Long, J. H. (1998). Muscles, elastic energy and the dynamics of body stiffness in swimming eels. *Am. Zool*. **38**, 771–792.

Lowe, R. H. (1952). The influence of light and other factors on the seaward migration of the silver eel (*Anguilla anguilla* L.). *J. Anim. Ecol.* **21**, 275–309.

Marey, E. J. (1895). *Movement*. London: Masson. 323pp.

McCleave, J. D. and Arnold, G. P. (1999). Movements of yellow- and silver-phase European eels (*Anguilla anguilla* L.) tracked in the western North Sea. *ICES J. Mar. Sci*. **56**, 510–536.

McCleave, J. D., Kleckner, R. C. and Castonguay, M. (1987). Reproductive sympatry of American and European eels and implications for migration and taxonomy. *Am. Fish. Soc. Symp.* **1**, 286–297.

Pankhurst, N. W. (1982). Changes in body musculature with sexual maturation in the European eel *Anguilla anguilla* (L.). *J. Fish Biol*. **21**, 417–428.

Parker, S. J. (1995). Homing ability and home range of yellow-phase American eels in a tidally dominated estuary. *J. Mar. Biol. Ass. U.K*. **75**, 127–140.

Poole, W. R., Reynolds, J. D. and Moriarty, C. (1990). Observations on the silver eel migrations of the Burrishoole River system, Ireland, 1959–1988. *Int. Rev. Ges. Hydrobiol.* **75**, 807–815.

Rayner, M. D. and Keenan, M. J. (1967). Role of red and white muscles in the swimming of the skipjack tuna. *Nature* **214**, 392–393.

Rome, L. C., Choi, I., Lutz, G. and Sosnicki, A. (1992). The influence of temperature on muscle function in the fast-swimming scup. I. Shortening velocity and muscle recruitment during swimming. *J. Exp. Biol*. **163**, 259–279.

Rome, L. C., Funke, R. P., Alexander, R. McN., Lutz, G.,

Aldridge, H., Scott, F. and Freadman, M. (1988). Why animals have different muscle fibres. *Nature* **355**, 824–827.

Rome, L. C., Swank, D. M. and Corda, D. (1993). How fish power swimming. *Science* **261**, 340–343.

Rome, L. C., Swank, D. M. and Coughlin, D. J. (2000). The influence of temperature on power production during swimming. II. Mechanics of red muscle fibres *in vitro*. *J. Exp. Biol*. **203**, 333–345.

Swank, D. M., Zhang, G. and Rome, L. C. (1997). Contraction kinetics of red muscle in scup: mechanism for relaxation rate along the length of the fish. *J. Exp. Biol*. **200**, 1297–1307.

van Leeuwen, J. L., Lankheet, M. J. M., Akster, H. A. and Osse, J. W. M. (1990). Function of red axial muscles in carp (*Cyprinus carpio* L.): recruitment and normalised power output during swimming in different modes. *J. Zool., Lond.* **220**, 123–145.

Vøllestad, L. A. and Jonsson, B. (1986). Life-history characteristics of the European eel *Anguilla anguilla* in the Imsa River, Norway. *Trans. Am. Fish. Soc.* **115**, 864–871.

Vøllestad, L. A., Jonsson, B., Hvidsten, N. A., Næsje, T. F., Haraldstad, Ø. and Ruud-Hansen, J. (1986). Environmental factors regulating the seaward migration of European silver eels (*Anguilla anguilla*). *Can. J. Fish. Aquat. Sci.* **43**, 1909–1916.

Wardle, C. S. and Videler, J. J. (1993). The timing of the electromyogram in the lateral myotomes of mackerel and saithe at different swimming speeds. *J. Fish Biol*. **42**, 347–359.

Wardle, C. S., Videler, J. J. and Altringham, J. D. (1995). Tuning in to fish swimming waves: body form, swimming mode and muscle function. *J. Exp. Biol*. **198**, 1629–1636.

Williams, G. C. and Koehn, R. K. (1984). Population genetics of North Atlantic catadromous eels (*Anguilla*). In *Evolutionary Genetics of Fishes* (ed. B. J. Turner), pp. 529–560. New York: Plenum.

Williams, T. L., Grillner, S., Smoljaninov, V. V., Wallen, P., Kashin, S. and Rossignol, S. (1989). Locomotion in lamprey and trout: the relative timing of activation and movement. *J. Exp. Biol*. **143**, 559–566.